Cryo-electron microscopy of membrane proteins

Goldie, Kenneth N ; Abeyrathne, Priyanka ; Kebbel, Fabian ; Chami, Mohamed ; Ringler, Philippe ; Stahlberg, Henning

Abstract: Electron crystallography is used to study membrane proteins in the form of planar, two-dimensional (2D) crystals, or other crystalline arrays such as tubular crystals. This method has been used to determine the atomic resolution structures of bacteriorhodopsin, tubulin, aquaporins, and several other membrane proteins. In addition, a large number of membrane protein structures were studied at a slightly lower resolution, whereby at least secondary structure motifs could be identified.In order to conserve the structural details of delicate crystalline arrays, cryo-electron microscopy (cryo-EM) allows imaging and/or electron diffraction of membrane proteins in their close-to-native state within a lipid bilayer membrane.To achieve ultimate high-resolution structural information of 2D crystals, meticulous sample preparation for electron crystallography is of outmost importance. Beam-induced specimen drift and lack of specimen flatness can severely affect the attainable resolution of images for tilted samples. Sample preparations that sandwich the 2D crystals between symmetrical carbon films reduce the beam-induced specimen drift, and the flatness of the preparations can be optimized by the choice of the grid material and the preparation protocol.Data collection in the cryo-electron microscope using either the imaging or the electron diffraction mode has to be performed applying low-dose procedures. Spot-scanning further reduces the effects of beam-induced drift. Data collection using automated acquisition schemes, along with improved and user-friendlier data processing software, is increasingly being used and is likely to bring the technique to a wider user base.

DOI: https://doi.org/10.1007/978-1-62703-776-1_15

Cryo-Electron Microscopy of Membrane Proteins

Kenneth N. Goldie, Priyanka Abeyrathne, Fabian Kebbel, Mohamed Chami, Philippe Ringler, and Henning Stahlberg

Center for Cellular Imaging and NanoAnalytics (C-CINA), Biozentrum, University Basel, Mattenstrasse 26, CH-4058 Basel, Switzerland

Corresponding Author:

Henning Stahlberg, Ph.D.

Center for Cellular Imaging and NanoAnalytics (C-CINA)

Biozentrum, University Basel

Mattenstrasse 26

CH-4058 Basel, Switzerland

Email: Henning.Stahlberg@unibas.ch

Tel.: +41-61-387 32 62. FAX: +41-61-387 39 86

Running Title: Cryo-EM of Membrane Proteins

Summary

Electron crystallography studies membrane proteins in form of planar, two-dimensional (2D) crystals, or other crystalline arrays such as tubular crystals. This method has been used to determine the atomic resolution structures of bacteriorhodopsin, tubulin, aquaporins, and several other membrane proteins. In addition, a large number of membrane protein structures were studied at a slightly lower resolution, whereby secondary structure motifs could be identified.

In order to conserve the structural details of delicate crystalline arrays, cryo-electron microscopy (cryo-EM) allows imaging and/or electron diffraction of membrane proteins in their close-to-native state within a lipid bilayer membrane.

To achieve ultimate high-resolution structural information of 2D crystals, meticulous sample preparation for electron crystallography is of outmost importance. Beam-induced specimen drift and lack of specimen flatness can severely affect the attainable resolution of images for tilted samples. Sample preparations that sandwich the 2D crystals between symmetrical carbon films reduce the beam-induced specimen drift, and the flatness of the preparations can be optimized by the choice of the grid material and the preparation protocol.

Data collection in the cryo-electron microscope using either the imaging or the electron diffraction mode has to be performed applying low-dose procedures. Spot scanning further reduces the effects of beam-induced drift. Data collection using automated acquisition schemes, along with improved and user-friendlier data processing software is increasingly being used and are likely to bring the technique to a wider user base.

Key Words: 2D membrane protein crystals; back-injection; sandwich method; spot-scanning; carbon flatness; low-dose; cryo-electron microscopy

1 Introduction

1.1 History

The foundations of electron crystallography and cryo-electron microscopy (cryo-EM) were laid in the early 1970's. The first structural determination of a biological unstained crystalline specimen was on purple membrane ***(1)***. This breakthrough required an understanding of the effects of drying on delicate samples, whereby glucose embedding was applied and the limitations from beam damage were overcome using low dose techniques at the microscope ***(2)***. Taylor and Glaeser ***(3)*** used electron diffraction of frozen, hydrated protein crystals, and also recorded images of samples preserved in a frozen hydrated state ***(4)***. The cryo-EM technique was further developed by the pioneering work of Dubochet and co-workers at the EMBL, where ethane was used as a cryogen to immobilize specimens in a vitreous ice state ***(5)***.

Structural biology of membrane proteins is of central importance in cellular biology and for the development of new drugs. Membrane proteins represent the majority of today's drug targets in pharmaceutical research. Enormous progress has been made in recent years in the structure determination of membrane proteins, whereby the majority of structures were determined by X-ray crystallography. Our databases now contain almost 400 unique folds of membrane proteins (http://blanco.biomol.uci.edu/mpstruc), and this number is growing almost exponentially. A remaining challenge is the understanding of the dynamic function of membrane proteins in the lipidic bilayer. Here, electron crystallography can provide significant insight into the conformation of membrane proteins in the membrane-embedded form. Two-dimensional membrane protein

crystals are stabilizing the membrane proteins in a lipid bilayer, and the surfaces of the proteins are readily accessible to ligands, changing buffer conditions, or binding partners.

1.2 Electron Crystallography

Electron crystallography studies the structure of membrane proteins in a two-dimensional crystalline arrangement in a phospholipid bilayer membrane. The atomic models of tubulin ***(6)*** and of the membrane proteins BR ***(7)***, LHCII ***(8)***, and water channels ***(9-13)***, were among the first membrane protein structures determined by electron crystallography at atomic resolution. Several other membrane proteins classified as transporters, ion pumps, receptors and membrane bound enzymes have been studied at slightly lower resolution allowing the localization of secondary structure motifs such as transmembrane helices ***(14)***.

Electron crystallography can be used to study membrane protein structures at resolutions of 3 Å or better (e.g., ***(11; 15; 16)***, demonstrating the value of this approach. Electron crystallography represents an alternative method for structure determination, when fragile membrane protein complexes cannot be grown into 3D protein crystals for X-ray diffraction, or are not available in sufficient quantities for NMR measurements. Information gleaned from EM reconstructions compliment X-ray diffraction data. EM preparations are often considered more physiologically relevant compared to crystals formed in the presence of detergents, as is sometimes the case with X-ray crystallography. Membrane-inserting proteins that undergo conformational changes between the soluble and the membrane-inserted state are likely to be best studied by electron crystallography. 2D membrane crystals are frequently grown easier than 3D crystals of membrane proteins, and offer to the membrane proteins a more native environment

than most 3D crystal forms. Membrane crystals are also advantageous for the structure determination of co-crystals, when pre-formed crystals are to be incubated with protein binding partners. Cryo-EM also offers the possibility to freeze-capture various protein conformational states as freezing rates in ethane ~10^6 °C/s ***(17)*** outperform the transient isomeric states (milliseconds) of proteins ***(18)***.

Technological advancements like the availability of coherent intermediate voltage electron sources and nitrogen or helium-cooled and stable sample stages ***(19)*** allow recording of high-resolution data of biological macromolecules. Improvement in detection devices such as CCD and CMOS cameras allow efficient data recording of electron diffraction patterns ***(20)***, and the advent of the first direct electron detection devices (DED) is likely to revolutionize also the imaging of 2D crystals. Advancements in sample preparation with the sandwich-back-injection technique using non-wrinkled carbon films ***(21-23)***, and the spot scanning data collection method ***(24)*** strongly reduce the resolution-limiting charge effect during data acquisition of tilted samples.

2D membrane protein crystallization usually requires detergent-solubilized and purified protein typically at a concentration of 1 mg/ml. Crystallization can be achieved by various methods ***(25-30)***. So far, the best-ordered 2D membrane protein crystals were obtained after slow and controlled detergent dialysis in the presence of added phospholipids ***(26)***. However, several other 2D crystallization methods were also developed ***(30-34)***.

2 Preparing 2D Crystals of Membrane Proteins for cryo-EM Analysis

This chapter describes the techniques and methods required for the structural analysis of 2D crystals by cryo-EM. Much effort must be invested to obtain large, single layered, well-ordered

crystals that are the starting point for our investigations. The expression, purification and crystallization of quality crystals is not covered in the context of this chapter but can be researched in other excellent reviews or books based on these specific themes ***(14; 30)***.

Grid sample preparation is equally as important as the operation of the electron microscope for the recording of high-resolution data of 2D crystal samples. The 2D crystalline arrangement of the sample allows efficient extraction of the structure's signal from extremely noisy images by computer processing. For the choice of the sample preparation, preference is therefore given to methods that perfectly preserve the high-resolution order of the 2D crystals, while the contrast characteristics of the preparation is of secondary importance.

Cryo-EM grids of 2D crystal samples can be prepared using holey or continuous carbon film support grids. However, holey carbon film coated grids, upon rapid plunge freezing, embed the samples in a thin (~100nm) layer of vitrified ice. This in most cases provides inferior electrical conductivity, physical stability and sample flatness compared to a continuous carbon film support ***(35)***. Grids for cryo-EM imaging of 2D crystals therefore usually employ continuous carbon film support. The following protocol describes the preparation of such grids.

2.1 Specimen Preparation

2.1.1 Materials

1. Carbon Evaporator (should have an oil-free high vacuum).
2. Mica sheets.
3. Petri dishes.

4. Anti-capillary self-closing tweezers.
5. Molybdenum TEM grids (e.g., 300 mesh Mo grids from Pacific Grid-Tech, TX, USA, ***(23)***, or holey carbon films (Quantifoil, Jena, Germany).
6. Humid chamber (home-made, constructed from Petri dishes).
7. Filter paper (Whatman, #1).
8. Liquid nitrogen in a Styrofoam cup, covered with aluminum foil to reduce boiling, for freezing of the sugar embedded grids.
9. For plunge freezing: A plunge freezer, if possible with a closed humid chamber (e.g., the Vitrobot, *see* http://www.fei.com/products/sample-prep/vitrobot.aspx; or a homebuilt device, *see* **Fig. 1**).
10. For the sandwich method: 4 mm diameter platinum wire loop (available for example from Ted Pella, Inc., Redding, CA, USA).

2.1.2 Plunge Freezing

2D crystals can be adsorbed to glow-discharged carbon-coated grids, blotted and plunge frozen (vitrified) in ethane slush, cooled by liquid nitrogen (*see* **Fig. 1**), similar to the preparation of cryo-EM grids with the holey carbon film method.

1. Evaporate carbon onto freshly cleaved mica (*see* **Note 1**).
2. Place mica with evaporated carbon into a humid chamber over night, to increase ease in floating the carbon off the mica.

3. Float carbon off the mica onto the surface of a buffer solution. This piece of carbon should be slightly larger than a TEM grid.
4. Pick up the carbon with a TEM grid (*see* **Note 2**).
5. Invert the tweezers with the grid upside down.
6. Remove a portion of the liquid on the grid with a pipette.
7. Add 1 to 3 microliter of 2D crystal solution (through the grid bars) (*see* **Note 3**).
8. Place the tweezers into a plunger (Guillotine).
9. Blot the grid with a filter paper and plunge-freeze in ethane slush (*see* **Note 4**).
10. Transfer the grid into a cryo-holder or microscope cartridge and image with minimal-dose (Low Dose) cryo-EM techniques.

2.1.3 Sugar Embedding (Back- injection)

Drying of membrane protein crystals in the presence of sugars such as tannic acid ***(8)***, trehalose ***(6; 36; 37)***, or glucose ***(15)*** can preserve the intact ultrastructure of the proteins, while eliminating the need for quick-freezing.

1. Evaporate carbon onto freshly cleaved mica (*see* **Note 1**).
2. Place mica with evaporated carbon into humid chamber over night, to ease floating the carbon off the mica, although in some cases this might not be necessary.
3. Float carbon off the mica onto the surface of a buffer solution.
4. Pickup the carbon with a TEM grid (*see* **Notes 2** and **5**).

5. Place the grid with the carbon film facing up onto three drops of sugar solution (*see* **Fig. 2B**; and also **Notes 6** and **7**).
6. Turn the tweezers with the grid upside down. The carbon film is now on the lower side of a hanging drop of sugar under the grid.
7. Remove a part of the liquid on the grid with a pipette (from the top through the grid bars) to level the solution surface on the grid.
8. Add 1 to 3 microliter of 2D crystal solution (1 mg/ml) through the grid bars (*see* **Note 3**).
9. Place grid in tweezers for 60 sec into a humid chamber, which can be constructed from three plastic Petri dishes (design by Dr. T. Braun, *see* **Fig. 2D**).
10. With a pipette, remove excess solution from the grid, leaving only about 1 microliter across the grid surface.
11. Turn the tweezers again upside down, and place the grid flat onto two layers of filter paper with the carbon film facing up (draining form the rear).
12. After sufficient blotting time (e.g., 20 sec), and subsequent freezing in liquid nitrogen, observe the grid in the TEM (*see* **Note 7**).

2.1.4 The Sandwich Method

The sandwich sample preparation method embeds the 2D crystals between two layers of carbon film. This preparation offers conductive surfaces one on each side of the sample, which may help reduce specimen charging. On the same time, this protocol presents a symmetrical sample structure to the electron beam, so that physical expansion during electron irradiation will

exert a symmetric lateral pressure, so that no unidirectional stress and movement can result from that. It may thereby increase the image stability under the electron beam ***(38)***. Another advantage of this method arises when it is used in conjunction with a staining solution, since it can provide a more even staining of the two sample surfaces, even though the second carbon film adds noise to the image (e.g., ***(39)***). The carbon sandwich can be made by placing both carbon films on the same surface of the TEM grid, resulting in the order grid->carbon->sample->carbon ***(39; 40)***. Alternatively, the two carbon films can cover both sides of the TEM grid, as described in ***(22)***, resulting in the order carbon->grid/sample->carbon. The latter is presented here:

1.-8. These steps are as above for Section 2.1.3 Sugar Embedding.

9. Float a second piece of carbon film onto buffer solution (*see* **Note 8**).

10. Lift the carbon film up with a 4mm diameter platinum wire loop and place it onto the grid from the top side, so that the grid and 2D crystals are sandwiched between the two carbon films (*see* **Fig. 3**).

11. Blot the sandwich construction from the edge of the grid, using a piece of torn filter paper.

12. Plunge the grid into liquid nitrogen manually by hand or with a plunge freezing device, and then transfer into the cryo-EM.

2.2 Electron Microscope Operation

Data collection on 2D crystals with the transmission electron microscope can be performed by recording either **images**, or **electron diffraction patterns**, or **both**. While the Fourier transformations of the images contain amplitudes *and* phases of the sample structure, electron

diffraction patterns allow a more reliable determination of the amplitudes, but lack the phase information.

2.2.1 Recording of Images

Image processing of images of 2D crystals with the crystallographic crystal unbending approach (described below) benefits from large image files of large 2D crystal areas. 2D crystal images were therefore usually recorded on photographic film, which was then digitized with a high-resolution scanner. So far, no CCD camera has produced high-resolution structures of membrane proteins. A new generation of scintillator-covered CMOS camera (e.g., as available from TVIPS, http://tvips.com) can now record images of 8192x8192 pixels at good detector quantum efficiency, and the new generation of direct electron detectors as available from FEI, Gatan, or Direct Electrons, also promises outstanding performances (e.g., ***(41)***).

The demands of high resolution imaging dictates that the electron microscope is well aligned with respect to gun and column alignments. These advanced alignments should be carried out by a highly trained engineer or qualified user. After eucentric specimen height adjustment, direct alignments should be applied prior to a data-set acquisition. Common alignments may include; aperture centering, pivot point correction, rotation and beam centering, along with coma-free alignment for optimal imaging conditions ***(42)***.

Recording of images of 2D crystals requires operation of the electron microscope under low-dose conditions, in which the microscope offers so-called “search”, “focus” and “exposure” positions. Choose a smaller second condenser aperture, and a larger objective aperture (~100 micrometers or larger). The latter may reduce specimen charging, due to a certain backscattering

of electrons onto the specimen. Align the TEM in the “exposure” position, then setup the “focus” position, and finally the “search” position. Cycle through the modes exclusively in the order “search” -> “focus” -> “exposure”, to prevent hysteresis effects that may make you loose the alignment.

1. Search position: The “search” position should allow easy localization of 2D crystal targets, which has to be done at very low illumination intensity. This can on some instruments best be achieved by observing the so-called shadow images, by setting the instrument up in a overfocussed electron diffraction mode. Use an electron diffraction camera length of 1 meter or longer. Set the second condenser lens to strong over-focus, to spread the illumination over a large sample area. Set the intermediate lens to over-focus, to create a strongly contrasted “shadow image” of the sample. Use a combination of image shift and beam tilt to align the center of the “search” position with the “exposure position”.

2. Focus position: The “focus” and the “exposure” position use the image mode of the electron microscope. In the “focus” position the instrument is operated under identical lens settings as used for the “exposure” position, but with additional beam- and image-shift, so that focusing the objective lens can be done adjacent to the sample location of interest. Align first the “exposure” position, then copy those settings to the “focus” position, and finally add sufficient beam- and image-shift so that the beam in the “focus” position does not illuminate the sample area of the “exposure” position. At 50 kx magnification, this usually corresponds to 3.5 micrometer beam deflection.

3. Exposure position: Images are recorded with the settings of the "exposure" position (e.g., 50'000x magnification, 0.5 seconds exposure time on a FEG instrument). Recorded images are modulated by the microscope's contrast transfer function (CTF), which can be corrected computationally. To reduce the number of Thon rings, try to work at lower defocus values, if the crystal quality is good enough. When images of tilted samples are recorded, a resolution loss in the direction perpendicular to the tilt axis can frequently be observed, resulting from charge-induced specimen drift and vibration of the sample. Images recorded on photographic film are best inspected by optical diffraction ***(43)*** before digitization.

Spot-scanning: When recording images of highly tilted samples, the resolution perpendicular to the tilt axis can be severely affected by beam-induced specimen drift during the acquisition. The illuminated sample area will react to the electron exposure by physical expansion and electrical charging, which can cause an upwards or downwards movement of the specimen, combined with a deflection of the electron beam ***(44)***. This effect can be minimized by the sandwich sample preparation method, but also by employing the so-called s*pot- scanning* illumination method ***(24)***: The electron beam on the sample is concentrated into an area of 50 to 200 nm diameter, and step-wise scanned over the sample area, while the entire hexagonally or alternatively shaped spot-scan pattern is recorded onto the same photographic film or detector (*see* **Fig. 4)**. Each *spot-scanning* spot has an exposure time of, for example 50 milliseconds (when using a FEG instrument), while the camera shutter remains open for a few minutes to record the entire *spot-scanning* pattern on one photographic film. Attention has to be paid to adjusting the illumination conditions so that central and off-axis *spot-scanning* spots have the same electron exposure without the introduction of excessive convergent illumination or off-axis beam tilt ***(42; 45)***.

2.2.2 Recording of Electron Diffraction Patterns

Electron diffraction patterns are not affected by the contrast transfer function of the microscope, nor by beam-tilt, nor suffer from specimen vibration or drift, and have only very limited dependence on specimen charging during the exposure. While electron diffraction usually requires well-ordered 2D crystal samples that are perfectly flat over an area more than a micrometer in diameter, its recording can be a time-efficient way to obtain a high-resolution amplitude dataset from tilted samples ***(46)***. Electron diffraction patterns are best recorded on a digital CCD or scintillator-covered CMOS camera, where the superior dynamic range (typically 12 to 16 bit) allows capturing intense low-resolution and weak high-resolution diffraction spots in a single exposure at good signal-to-noise ratio ***(47)***. Depending on the unit cell spacing of the 2D crystal and the expected resolution in a diffraction pattern, a digital camera of 2048 x 2048 or higher pixel number is required, to sufficiently resolve individual diffraction spots in a diffraction pattern ***(47)***.

To record diffraction patterns, all positions of the low-dose system are setup in diffraction mode. Choose a small second condenser aperture of 10 or 20 micrometers diameter, and remove the objective aperture. If a diffraction aperture is present it can be inserted to reduce the beam area exposed.

1. Search position: The “search” position is set-up as described above, using the “shadow” image of the over-focused diffraction mode with an over-focused second condenser lens and over-focused intermediate lens.

2. Focus position: Usage of this position is optional and may not be required, if the microscope is sufficiently stable, since the electron diffraction focus does not depend on the sample position or sample height. The "focus" position is a copy of the "exposure" position and therefore also uses the electron diffraction mode. Focusing is done *on* the sample. The "focus" mode does not use additional beam or image shift. The alignments of the "exposure" and the "focus" mode only differ in illumination system settings: A highly excited first condenser lens in the "focus" position is used to dim the sample illumination to the lowest possible intensity. The second (and/or third) condenser lens is then adjusted to again achieve parallel illumination onto the sample. Focusing the diffraction pattern with the intermediate lens can then be done by focusing the *direct* (zero-order) beam on the screen. The focusing settings from the "focus" position are only valid for the "exposure" position, if both "focus" and "exposure" positions are using the identical illumination conditions onto the sample, which can be verified by checking if the objective aperture border appears sharp in both modes. (This requires the objective aperture to be aligned to the correct height, which is the back-focal plane of the objective lens. Don't forget to remove the objective aperture from the beam for recording the diffraction pattern).

3. Exposure position: In the "exposure" position, the diffraction pattern of the crystalline sample is recorded, using a long exposure time (e.g., 30 sec or longer). This position has to provide an alignment with parallel illumination of the sample. Recording of electron diffraction pattern can be done with or without a "selected area diffraction" (SAD) aperture. If you chose to limit the electrons that contribute to the diffraction pattern

4. Using a SAD aperture, you can illuminate a sample area somewhat larger than the diffracting crystal, allowing a more coherent and homogeneous illumination of the crystal.

The dose for recording one image should be in the order of 500 electrons/nm^2 at liquid nitrogen temperature but can be as high as 2000 electrons/nm^2 at liquid helium temperature for trehalose-embedded samples, when information in the resolution range beyond 4 Å is to be recorded. Observations of changes in electrical conductivity, viscosity, and density of vitreous ice at liquid helium temperatures ***(48-50)*** might not apply to phospholipid bilayers and/or sugar-embedded samples, which would explain why for 2D crystal samples the usage of helium-cooled instruments has proven strongly beneficial ***(51)***.

2.3 Computer Image Processing

The recorded images and diffraction patterns contain the high-resolution information about the structure of the membrane proteins. However, due to the low electron-optical density differences between membrane proteins and the surrounding lipids, and due to the usually quite low molecular weights of the membrane proteins, these images are not interpretable by the naked eye. Instead, extensive computer image processing is necessary, to extract the contained information from the very noisy datasets.

Image processing of 2D crystal cryo-EM data can be done with various software packages. Historically, the so-called MRC software, created by Richard Henderson and co-workers in the MRC, Cambridge, UK, offers a mathematically powerful implementation of various tools for the unending of crystal lattice distortions, and the Fourier space extraction of values for Amplitudes and Phases of the membrane protein structures ***(1; 7; 52-54)***. The *2dx* software package is based

on these MRC programs, and offers a graphical user interface that allows to interact with the MRC programs in a user-friendly and well documented way, while in addition offering various functions for the streamlining or optional full automation of the 2D crystal image processing workflow ***(55-58)***. In addition, the *2dx* package includes modules for a single-particle processing of 2D crystal images, which is advantageous for the processing of images of non-perfectly ordered or non-flat 2D crystals ***(59)***. In addition, *2dx* offers user-guidance and optionally fully automatic processing of 2D crystal images. *2dx* provides the user with an intuitive system for data management, default processing parameters and a broad documentation integrated in the front end.

For the processing of electron diffraction data, the MRC software package offers robust programs that automatically index diffraction patterns and evaluate the data from those patterns. The XDP software tool ***(16)*** can be used to facilitate the use of the MRC programs by adding a front-end software system for diffraction pattern evaluation.

A new development for electron crystallography data processing for images and diffraction patterns is IPLT ***(60; 61)***, a package that does not make use of the MRC software suite, but provides a reimplementation of existing algorithms as well as newly developed algorithms for 2d crystal processing in a modular way.

These software systems were recently comparatively evaluated ***(62)***. A comprehensive manual for the image processing can be found in the book “Electron Crystallography of Soluble and Membrane Proteins”, edited by Ingeborg Schmidt-Krey and Yifan Cheng ***(63)***, where several chapters discuss the processing of 2D crystal images, and the various algorithms, steps and tricks involved ***(64-66)***.

3 Notes

1. The flatness of the supporting carbon film is of high importance when attempting to record images at high resolution. This is especially important, when images of tilted 2D crystal samples are to be recorded, since small tilt-angle variations will strongly affect the resolution perpendicular to the tilt axis ***(67)***. Uneven or rough carbon film can perturb the specimen flatness, which also can be severely affected by so-called cryo-crinkling of the carbon film ***(22; 23; 68)*** due to different thermal expansion coefficients between the sample and the support grid. Carbon film is usually prepared by carbon evaporation onto freshly cleaved mica, which should be done at a vacuum better than 5 x 10^{-6} mbar. Care should be taken that only carbon films from evaporation processes without sparking are used. Carbon films prepared in this way will be smoother on the mica-facing side than on the carbon source-facing side ***(69)***. Therefore, the 2D crystal samples should be adsorbed onto the side of the carbon film, which previously was facing the mica.

2. Carbon film should be floated onto the darker, less shiny side of the TEM support grid, which will attach better to the carbon film and result in smoother films ***(23)***. Cryo-crinkling can be reduced significantly by utilizing grid materials with thermal expansion coefficients similar to that of the sample: Cryo-crinkling is strongest with copper, less with titanium and best with molybdenum grids ***(21; 70)***. Although not generally recommended, costly molybdenum grids may be re-used after ultrasound cleaning in ethanol. Carbon film will rupture less often, when using grids with a greater

number or thicker, metal bars, but the visible sample area on tilted grids will be smaller, and the amount of cryo-crinkling will increase ***(23)***. For high-resolution imaging, 300 mesh molybdenum grids are recommended.

3. The spreading of 2D crystals onto the carbon film can be facilitated by the addition of small amounts of detergents. Bacitracin (0.25 mg/ml) in the sugar solution can for example be used as wetting agent to help increase spreading ***(71)***. In addition, a pipette can be used to take up a part of the sample/sugar solution at the edge of the grid, and re-admit it to the center of the grid several times, to physically increase spreading of the crystals onto the carbon film. Spreading can also improve if longer adsorption times are allowed. This requires the availability of a humidity chamber to prevent sample evaporation during the adsorption time of a few min.

4. The sample solution does not evaporate as rapidly on a continuous carbon film as it would do on holey carbon film, allowing longer blotting times. While electrical charging of ice contamination on the grid is more difficult to control with this method, vitrification by plunge freezing of 2D crystals on a continuous carbon film may be preferred over sugar embedding, when good contrast of undisturbed protein surface structures is required.

5. This is best done by holding the grid with self-closing inverted anti-capillary tweezers.

6. The grid is placed for a few seconds onto three drops of buffer solution containing 1 to 7% (w/v) of sugar (e.g., trehalose, glucose, tannic acid), in order to replace the water under the carbon film with the sugar solution (*see* **Fig. 2C**). To maintain an intact

carbon film, attention has to be paid to avoid wetting the carbon film on the upper surface.

7. Many membrane protein 2D crystals support complete drying in glucose, without loss of intrinsic high-resolution order. A grid with a glucose-embedded sample can usually be dried extensively, and even be loaded with a cryo-sample holder into the vacuum of the TEM, while still at room temperature. The grid quality can then be assessed at room temperature in the TEM, which on most microscopes is faster than handling a cryo-grid at low temperatures. Only after verifying that the grid shows a suitable sample density and glucose thickness, the cryo-EM holder is filled with liquid nitrogen to cool the sample. This sample preparation results in cryo-grids that initially are completely free of ice contamination from the grid transfer. Trehalose embedded membrane proteins will in most cases still require the presence of traces of water. A grid prepared with trehalose should therefore only be blotted for ~20 sec (depending on air humidity), and then frozen by manual plunging into liquid nitrogen. Since trehalose prevents ice crystal formation, quick-freezing in ethane slush is not necessary. The grid can then be mounted into a pre-cooled cryo-sample holder and transferred into the TEM.

8. The second piece of carbon film should be slightly smaller than the grid. To yield a symmetrical carbon film sandwich, this second carbon film should be from the same evaporation process as the first. The symmetrical carbon is essential to reduce the beam-induced specimen drift (Y. Fujiyoshi, personal communication, 2004, and ***(68)***.

4 References

1. Henderson R, and Unwin PN (1975) Three-dimensional model of purple membrane obtained by electron microscopy. Nature ***257***, 28-32.
2. Unwin PN, and Henderson R (1975) Molecular structure determination by electron microscopy of unstained crystalline specimens. J Mol Biol ***94***, 425-440.
3. Taylor KA, and Glaeser RM (1974) Electron diffraction of frozen, hydrated protein crystals. Science ***186***, 1036-1037.
4. Taylor KA, and Glaeser RM (1976) Electron microscopy of frozen hydrated biological specimens. J Ultrastruct Res ***55***, 448-456.
5. Adrian M, Dubochet J, Lepault J, and McDowall AW (1984) Cryo-electron microscopy of viruses. Nature ***308***, 32-36.
6. Nogales E, Wolf SG, and Downing KH (1998) Structure of the alpha beta tubulin dimer by electron crystallography. Nature ***391***, 199-203.
7. Henderson R, Baldwin JM, Ceska TA, Zemlin F, Beckmann E, and Downing KH (1990) Model for the structure of *Bacteriorhodopsin* based on high-resolution electron cryo-microscopy. J Mol Biol ***213***, 899- 929.
8. Kühlbrandt W, Wang DN, and Fujiyoshi Y (1994) Atomic model of plant light-harvesting complex by electron crystallography. Nature ***367***, 614-621.
9. Murata K, Mitsuoka K, Hirai T, Walz T, Agre P, Heymann JB, Engel A, and Fujiyoshi Y (2000) Structural determinants of water permeation through aquaporin-1. Nature ***407***, 599-605.
10. Ren G, Reddy VS, Cheng A, Melnyk P, and Mitra AK (2001) Visualization of a water-selective pore by electron crystallography in vitreous ice. Proc Natl Acad Sci U S A ***98***, 1398-1403.
11. Gonen T, Sliz P, Kistler J, Cheng Y, and Walz T (2004) Aquaporin-0 membrane junctions reveal the structure of a closed water pore. Nature ***429***, 193-197.
12. Hiroaki Y, Tani K, Kamegawa A, Gyobu N, Nishikawa K, Suzuki H, Walz T, Sasaki S, Mitsuoka K, Kimura K, *et al*. (2006) Implications of the aquaporin-4 structure on array formation and cell adhesion. J Mol Biol ***355***, 628-639.
13. Tani K, Mitsuma T, Hiroaki Y, Kamegawa A, Nishikawa K, Tanimura Y, and Fujiyoshi Y (2009) Mechanism of aquaporin-4's fast and highly selective water conduction and proton exclusion. J Mol Biol ***389***, 694-706.
14. Abeyrathne PD, Arheit M, Kebbel F, Castano-Diez D, Goldie KN, Chami M, Renault R, Kühlbrand W, and Stahlberg H (2012). Electron microscopy analysis of 2D Crystals of membrane proteins. In Comprehensive Biophysics, E.H. Egelman, ed. (Academic Press), pp. 277-310.
15. Grigorieff N, Ceska TA, Downing KH, Baldwin JM, and Henderson R (1996) Electron-Crystallographic Refinement of the Structure of Bacteriorhodopsin. J Mol Biol ***259***, 393-421.
16. Mitsuoka K, Hirai T, Murata K, Miyazawa A, Kidera A, Kimura Y, and Fujiyoshi Y (1999) The structure of bacteriorhodopsin at 3.0 Å resolution based on electron crystallography: Implication of the charge distribution. J Mol Biol ***286***, 861.

17. Dubochet J, Adrian M, Chang JJ, Homo JC, Lepault J, McDowall AW, and Schultz P (1988) Cryo-electron microscopy of vitrified specimens. [Review]. Quart Rev Biophys ***21***, 129-228.
18. Fujiyoshi Y, and Unwin N (2008) Electron crystallography of proteins in membranes. Curr Opin Struct Biol ***18***, 587-592.
19. Fujiyoshi Y, Mizusaki T, Morikawa K, Yamagishi H, Aoki Y, Kihara H, and Harada Y (1991) development of a superfluid helium stage for high resolution electron microscopy. Ultramicroscopy ***38***, 241-251.
20. Downing KH, and Hendrickson FM (1999) Performance of a 2k CCD camera designed for electron crystallography at 400 kV. Ultramicroscopy ***75***, 215-233.
21. Glaeser RM (1992) Specimen flatness of thin crystalline arrays: influence of the substrate. Ultramicroscopy ***46***, 33-43.
22. Gyobu N, Tani K, Hiroaki Y, Kamegawa A, Mitsuoka K, and Fujiyoshi Y (2004) Improved specimen preparation for cryo-electron microscopy using a symmetric carbon sandwich technique. J Struct Biol ***146***, 325-333.
23. Vonck J (2000) Parameters affecting specimen flatness of two-dimensional crystals for electron crystallography. Ultramicroscopy ***85***, 123-129.
24. Downing KH (1991) Spot-scan imaging in transmission electron microscopy. Science ***251***, 53-59.
25. Remigy HW, Caujolle-Bert D, Suda K, Schenk A, Chami M, and Engel A (2003) Membrane protein reconstitution and crystallization by controlled dilution. FEBS Lett ***555***, 160-169.
26. Jap BK, Zulauf M, Scheybani T, Hefti A, Baumeister W, Aebi U, and Engel A (1992) 2D crystallization: from art to science. Ultramicroscopy ***46***, 45-84.
27. Levy D, Chami M, and Rigaud JL (2001) Two-dimensional crystallization of membrane proteins: the lipid layer strategy. FEBS Lett ***504***, 187-193.
28. Kühlbrandt W (1992) Two-dimensional crystallization of membrane proteins. Quart Rev Biophys ***25***, 1-49.
29. Hasler L, Heymann JB, Engel A, Kistler J, and Walz T (1998) 2D crystallization of membrane proteins: rationales and examples. J Struct Biol ***121***, 162-171.
30. Abeyrathne PD, Chami M, Pantelic RS, Goldie KN, and Stahlberg H (2010) Preparation of 2D crystals of membrane proteins for high-resolution electron crystallography data collection. Methods Enzymol ***481***, 25-43.
31. Signorell GA, Kaufmann TC, Kukulski W, Engel A, and Remigy HW (2007) Controlled 2D crystallization of membrane proteins using methyl-beta-cyclodextrin. J Struct Biol ***157***, 321-328.
32. Iacovache I, Biasini M, Kowal J, Kukulski W, Chami M, van der Goot FG, Engel A, and Remigy HW (2010) The 2DX robot: a membrane protein 2D crystallization Swiss Army knife. J Struct Biol ***169***, 370-378.
33. Coudray N, Hermann G, Caujolle-Bert D, Karathanou A, Erne-Brand F, Buessler JL, Daum P, Plitzko JM, Chami M, Mueller U, *et al.* (2011) Automated screening of 2D crystallization trials using transmission electron microscopy: a high-throughput tool-chain for sample preparation and microscopic analysis. J Struct Biol ***173***, 365-374.

34. Hu M, Vink M, Kim C, Derr K, Koss J, D'Amico K, Cheng A, Pulokas J, Ubarretxena-Belandia I, and Stokes D (2010) Automated electron microscopy for evaluating two-dimensional crystallization of membrane proteins. J Struct Biol ***171***, 102-110.
35. Henderson R (1992) Image contrast in high-resolution electron microscopy of biological macromolecules: TMV in ice. Ultramicroscopy ***46***, 1-18.
36. Kimura Y, Vassylyev DG, Miyazawa A, Kidera A, Matsushima M, Mitsuoka K, Murata K, Hirai T, and Fujiyoshi Y (1997) Surface of bacteriorhodopsin revealed by high-resolution electron crystallography. Nature ***389***, 206-211.
37. Murata K, Mitsuoka K, Hirai T, Walz T, Agre P, Heymann JB, Engel A, and Fujiyoshi Y (2000) Structural determinants of water permeation through aquaporin-1. Nature ***407***, 599-605.
38. Glaeser RM (2008) Retrospective: radiation damage and its associated "information limitations". J Struct Biol ***163***, 271-276.
39. Golas MM, Sander B, Will CL, Luhrmann R, and Stark H (2003) Molecular architecture of the multiprotein splicing factor SF3b. Science ***300***, 980-984.
40. Golas MM, Sander B, Will CL, Luhrmann R, and Stark H (2005) Major conformational change in the complex SF3b upon integration into the spliceosomal U11/U12 di-snRNP as revealed by electron cryomicroscopy. Molecular cell ***17***, 869-883.
41. Bai X-C, Fernandez IS, McMullan G, and Scheres SH (2013) Ribosome structures to near-atomic resolution from thirty thousand cryo-EM particles. eLife ***in press***.
42. Glaeser RM, Typke D, Tiemeijer PC, Pulokas J, and Cheng A (2011) Precise beam-tilt alignment and collimation are required to minimize the phase error associated with coma in high-resolution cryo-EM. J Struct Biol ***174***, 1-10.
43. Aebi U, Smith PR, Dubochet J, Henry C, and Kellenberger E (1973) A study of the structure of the T-layer of *Bacillus brevis*. J Supramol Struct ***1***, 498-522.
44. Glaeser RM, and Hall RJ (2011) Reaching the information limit in cryo-EM of biological macromolecules: experimental aspects. Biophys J ***100***, 2331-2337.
45. Zhang X, and Zhou ZH (2011) Limiting factors in atomic resolution cryo electron microscopy: no simple tricks. J Struct Biol ***175***, 253-263.
46. Walz T, and Grigorieff N (1998) Electron Crystallography of Two-Dimensional Crystals of Membrane Proteins. J Struct Biol ***121***, 142-161.
47. Downing KH, and Li H (2001) Accurate recording and measurement of electron diffraction data in structural and difference Fourier studies of proteins. Microscopy and microanalysis : the official journal of Microscopy Society of America, Microbeam Analysis Society, Microscopical Society of Canada ***7***, 407-417.
48. Iancu CV, Wright ER, Heymann JB, and Jensen GJ (2006) A comparison of liquid nitrogen and liquid helium as cryogens for electron cryotomography. J Struct Biol ***153***, 231-240.
49. Comolli LR, and Downing KH (2005) Dose tolerance at helium and nitrogen temperatures for whole cell electron tomography. J Struct Biol, (in press).
50. Bammes BE, Jakana J, Schmid MF, and Chiu W (2010) Radiation damage effects at four specimen temperatures from 4 to 100 K. J Struct Biol ***169***, 331-341.
51. Fujiyoshi Y (1998) The structural study of membrane proteins by electron crystallography. Adv Biophys ***35***, 25-80.

52. Amos LA, Henderson R, and Unwin PN (1982) Three-dimensional structure determination by electron microscopy of two-dimensional crystals. Prog Biophys Mol Biol ***39***, 183-231.
53. Henderson R, Baldwin JM, Downing KH, Lepault J, and Zemlin F (1986) Structure of purple membrane from *Halobacterium halobium* : recording, measurement and evaluation of electron micrographs at 3.5 Å resolution. Ultramicroscopy ***19***, 147-178.
54. Crowther R, Henderson R, and Smith J (1996) MRC image processing programs. J Struct Biol ***116***, 9-16.
55. Gipson B, Zeng X, Zhang Z, and Stahlberg H (2007) 2dx—User-friendly image processing for 2D crystals. J Struct Biol ***157***, 64-72.
56. Gipson B, Zeng X, and Stahlberg H (2008) 2dx - Automated 3D structure reconstruction from 2D crystal data. Microscopy and Microanalysis ***14***, 1290-1291.
57. Gipson B, Zeng X, and Stahlberg H (2007) 2dx_merge: data management and merging for 2D crystal images. J Struct Biol ***160***, 375-384.
58. Zeng X, Gipson B, Zheng ZY, Renault L, and Stahlberg H (2007) Automatic lattice determination for two-dimensional crystal images. J Struct Biol ***160***, 353-361.
59. Zeng X, Stahlberg H, and Grigorieff N (2007) A maximum likelihood approach to two-dimensional crystals. J Struct Biol ***160***, 362-374.
60. Philippsen A, Schenk AD, Signorell GA, Mariani V, Berneche S, and Engel A (2007) Collaborative EM image processing with the IPLT image processing library and toolbox. J Struct Biol ***157***, 28-37.
61. Philippsen A, Schenk AD, Stahlberg H, and Engel A (2003) Iplt--image processing library and toolkit for the electron microscopy community. J Struct Biol ***144***, 4-12.
62. Schenk AD, Castano-Diez D, Gipson B, Arheit M, Zeng X, and Stahlberg H (2010) 3D reconstruction from 2D crystal image and diffraction data. Meth Enzymol ***482***, 101-129.
63. Schmidt-Krey I, and Cheng Y, eds. (2013). Electron crystallography of soluble and membrane proteins (New York, Humana Press).
64. Arheit M, Castano-Diez D, Thierry R, Abeyrathne P, Gipson BR, and Stahlberg H (2013) Merging of image data in electron crystallography. Methods Mol Biol ***955***, 195-209.
65. Arheit M, Castano-Diez D, Thierry R, Gipson BR, Zeng X, and Stahlberg H (2013) Automation of image processing in electron crystallography. Methods Mol Biol ***955***, 313-330.
66. Arheit M, Castano-Diez D, Thierry R, Gipson BR, Zeng X, and Stahlberg H (2013) Image processing of 2D crystal images. Methods Mol Biol ***955***, 171-194.
67. Glaeser RM, and Downing KH (1992) Assessment of resolution in biological electron crystallography. Ultramicroscopy ***47***, 256-265.
68. Glaeser RM, and Downing KH (2004) Specimen charging on thin films with one conducting layer: discussion of physical principles. Microscopy and microanalysis : the official journal of Microscopy Society of America, Microbeam Analysi ***10***, 790-796.
69. Butt H-J, Wang DN, Hansma PK, and Kühlbrandt W (1991) Effect of surface roughness of carbon support films on high-resolution electron diffraction of two-dimensional protein crystals. Ultramicroscopy ***36***, 307-318.
70. Booy FP, and Pawley JB (1993) Cryo-crinkling: what happens to carbon films on copper grids at low temperature. Ultramicroscopy ***48***, 273-280.

71. Mindell JA, Maduke M, Miller C, and Grigorieff N (2001) Projection structure of a ClC-type chloride channel at 6.5 Å resolution. Nature ***409***, 219-223.
72. Schenk AD, Werten PJ, Scheuring S, de Groot BL, Müller SA, Stahlberg H, Philippsen A, and Engel A (2005) The 4.5 Å structure of human AQP2. J Mol Biol ***350***, 278-289.

5 Figures

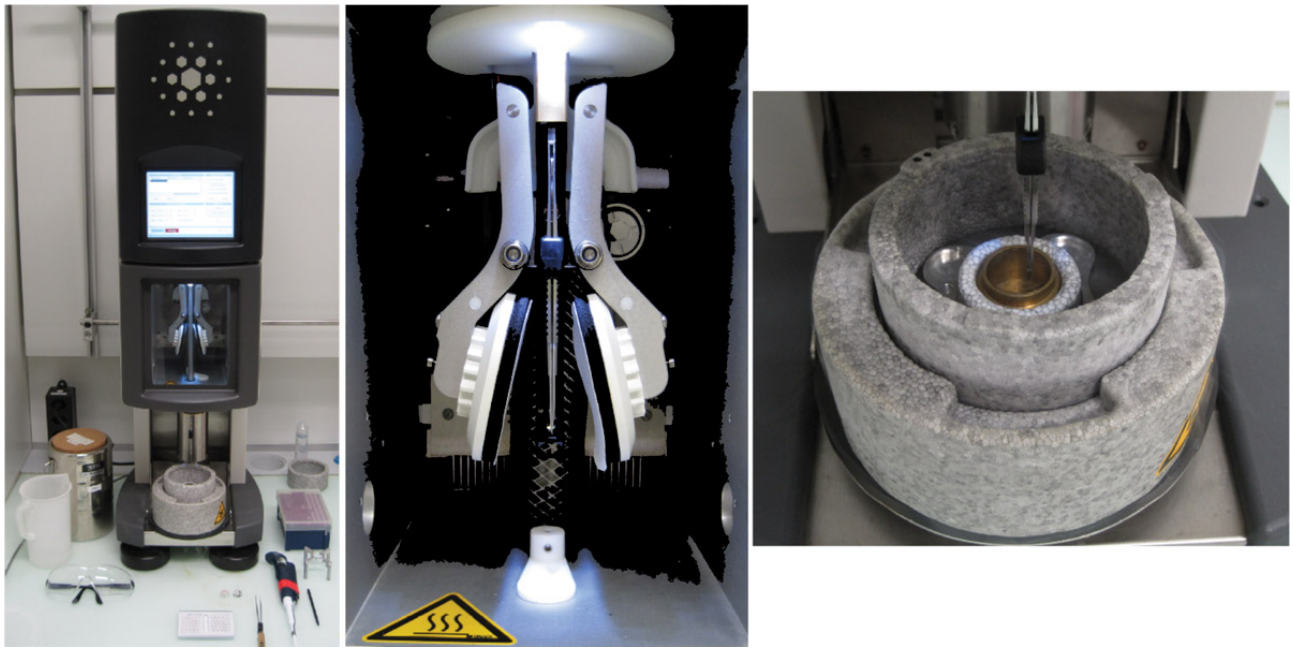

Fig. 1. The plunge-freezing device; FEI Vitrobot fitted with a humidity and temperature controlled chamber. The grid is held by tweezers in the center of the device (left). Sample can be added through an opening aperture on either side of the sample chamber (middle). After a pre-determined incubation time, blotting is carried out automatically by filter paper blotting pads mounted on pivoting levers at each side of the sample. After a set blotting time (blotting pressure is also adjustable) the sample held by forceps is rapidly plunged into LN_2-cooled ethane liquid or slush. The liquid ethane/nitrogen container is mounted directly below the specimen chamber during plunging and moves down for transfer of the grid to a suitable grid box (right). The sample must be kept in cold nitrogen, below the de-vitrification temperature ≈ -150°C, throughout the process and during transfer to a grid storage box. The frozen sample can then be stored under LN_2 until ready for viewing in the TEM.

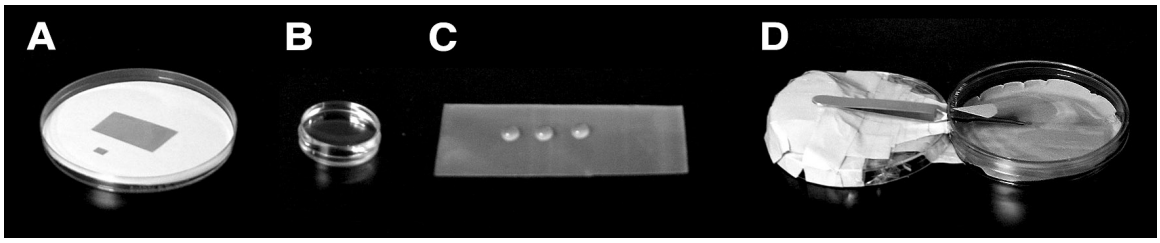

Fig. 2. Sugar embedding of 2D crystals requires a piece of carbon the size of a grid. This can be cut from mica with evaporated carbon (**A**). The carbon is floated onto a water surface (**B**) and placed onto three drops of sugar containing buffer solution (**C**). After adding the crystal solution, the grid is allowed to rest for a few minutes in a humid atmosphere that can be created using Petri dishes (**D**). The edge of the cover of the right Petri dish was broken off over a stretch of 2 cm, forming a hole where the tip of the tweezers can enter. The bottom of the right Petri dish is covered with a wet filter paper, which increases air humidity when the Petri dish is closed.

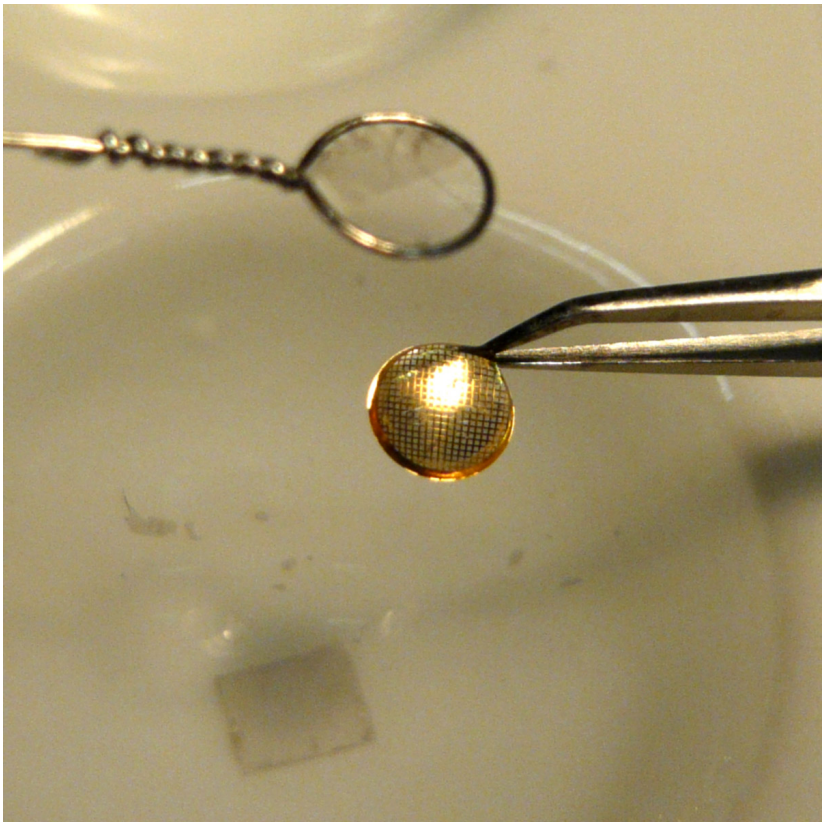

Fig. 3. Transfer of the second carbon film onto the grid to form the carbon film sandwich. The grid holds a carbon film at its lower side, onto which the 2D crystal sample has been adsorbed. The platinum loop is used to transfer a second carbon film onto the grid from the top, forming a carbon sandwich that surrounds the 2D crystals.

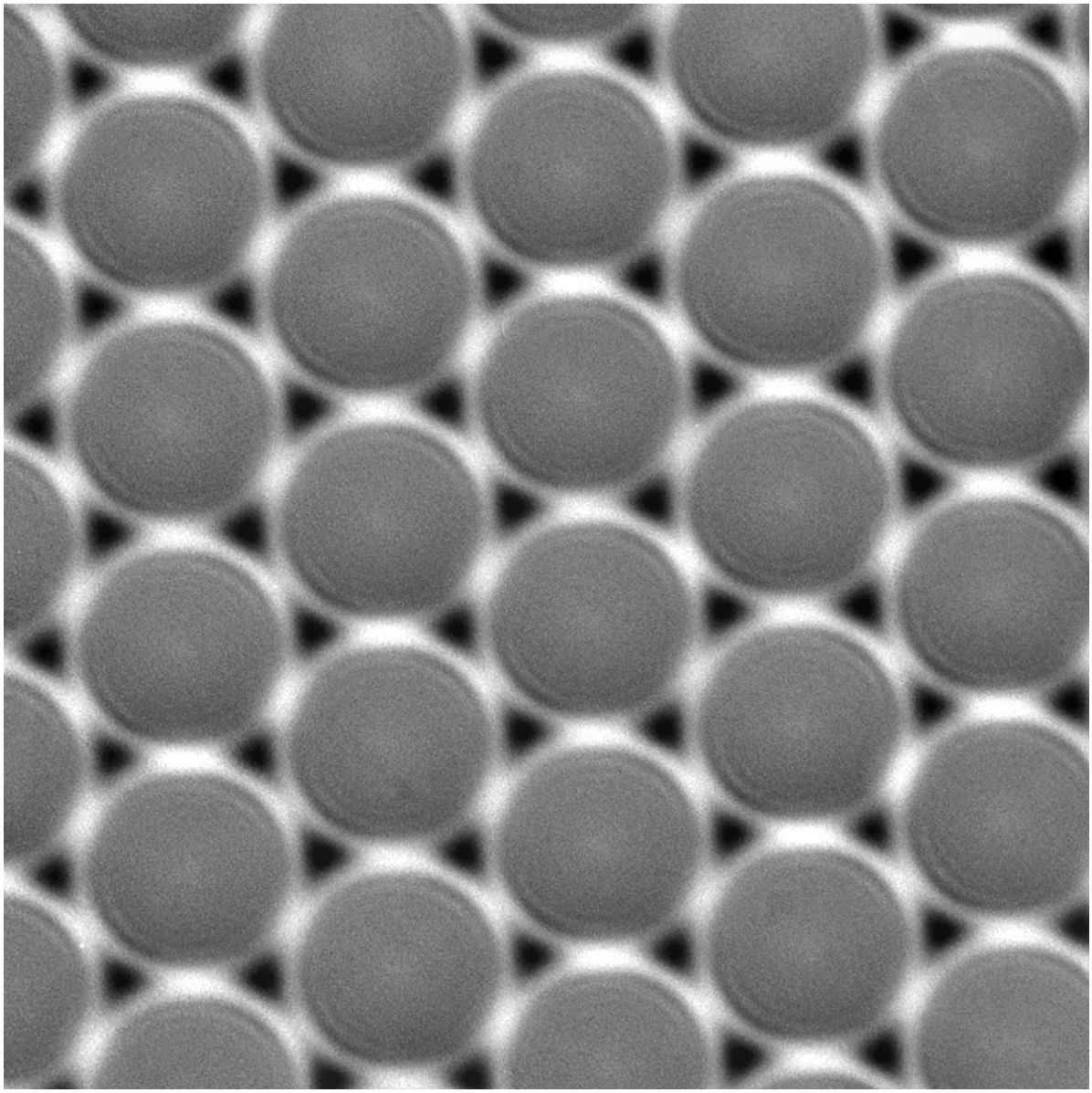

Fig. 4. A micrograph recorded by spot scanning of AQP2 2D crystals ***(72)***. The ~100 nm diameter spots cover in a hexagonal pattern, the micrograph, which in total spans an area of ~0.6 μm square (dimensions on the sample level). The finer AQP2 2D crystal lattice is not recognizable in the unprocessed image. Such an image can be computer processed to mask the non-exposed dark triangles and the double-exposed bright contact edges between the spot-scan spots, and replace these regions with the average grey value.